v1: 9 May 2025

Research Article

Impact of Carrier Leakage on NavIC Signal Performance

Peer-approved: 9 May 2025

Qeios, Vol. 7 (2025)
ISSN: 2632-3834

Deepak Mishra[1], Neeraj Mishra[1], Harsh Agarwal[1]

1. Indian Space Research Organisation, Bengaluru, India

Homodyne-based digital modulators are widely used in navigation satellite systems, such as in the Navigation with Indian Constellation (NavIC). In these systems, the mixer plays a crucial role by up-converting zero-IF complex modulated signals to the desired carrier frequency. However, insufficient port-to-port isolation in the mixer can cause leakage of the local oscillator (LO) carrier into the output, resulting in unwanted in-band signals within the transmitted spectrum. When these leaked signals are amplified by transmit filters and onboard high-power amplifiers, they distort the transmitted navigation signals, impairing system performance.

Traditional analytical methods for assessing interference in Global Navigation Satellite Systems (GNSS) often assume ideal signal conditions, mainly focusing on intersystem and intrasystem interference. This paper extends the current interference analysis framework by integrating the effects of carrier leakage and other imperfections specific to homodyne transmitter designs.

We introduce a system model for a homodyne transmitter and provide a mathematical representation of the NavIC interplex signal, including in-band carrier leakage. The impact of these imperfections is analyzed by examining the degradation in the effective carrier-to-noise ratio (C/No) and the data demodulation thresholds at the receiver.

The proposed methodology allows for a more accurate and practical evaluation of NavIC receiver performance, facilitating improved optimization of modulator designs and effective interference mitigation strategies. These findings are vital for enhancing the robustness and accuracy of NavIC services and advancing efficient GNSS operations in various environments.

Deepak Mishra, Neeraj Mishra, and Harsh Agarwal contributed equally to this work.

Corresponding author: Deepak Mishra, deepakmishra@sac.isro.gov.in

1. Introduction

Global Navigation Satellite Systems (GNSS) have revolutionized navigation and positioning capabilities across various applications. These systems, which include GPS, GLONASS, Galileo, BeiDou, and NavIC, rely on satellite constellations to provide global or regional Positioning, Navigation, and Timing (PNT) services[1][2]. GNSS satellites operate in Medium Earth Orbit (MEO) and Geostationary/Geosynchronous Earth Orbit (GEO), transmitting navigation signals that allow ground-based receivers to accurately determine Position, Velocity and Time (PVT) solutions[3].

India's Navigation with Indian Constellation (NavIC) is a regional satellite navigation system designed to offer precise positioning and timing services in the Indian subcontinent and surrounding areas. With a constellation of seven satellites in geostationary and geosynchronous orbits, NavIC ensures reliable coverage for civilian and military applications. Recent advances, including the introduction of new generation of navigation satellite systems (NVS), aims to enhance signal strength, accuracy, and overall system robustness. NavIC offers two services: the Standard Positioning Service (SPS) for civilian users and a Restricted Service for authorized users. It transmits

 doi.org/10.32388/U517J4.3

signals in the L1-Band (1575.42 MHz), S-band (2492.028 MHz) and the L5 band (1176.45 MHz)[4][5].

The growing use of frequency bands by multiple GNSS systems has resulted in increased intrasystem and intersystem interference, posing significant challenges to navigation performance. In addition, the introduction of new signals to improve GNSS services has intensified congestion within the radio frequency spectrum. Therefore, comprehensive analysis is essential to mitigate interference and ensure reliable system performance[6][7][8].

Among the signal imperfections that affect the performance of the GNSS receiver, carrier leakage, also known as ”incompletely suppressed carrier,” is particularly notable. This issue manifests itself as a sharp spectral spike at the center of the transmitted signal due to inadequate suppression of the local oscillator (LO) carrier in transmitter designs. Carrier leakage diverts transmitter power, leading to reduced effective signal power, a degradation in the carrier-to-noise ratio (C/N_0), and increased range biases[9]. Historical examples, such as the 1993 GPS PRN 19 failure and the 2012 BeiDou GEO-3 anomaly, highlight the operational risks associated with carrier leakage[10][11].

Carrier leakage is a specific form of continuous-wave interference (CWI) and can exacerbate interference challenges within and between GNSS systems. Despite advancements in transmitter design, residual leakage remains a concern, contributing to in-band interference that distorts navigation signals. Analytical metrics, such as the Signal-to-Noise plus Interference Ratio (SNIR) and Spectral Separation Coefficient (SSC), are crucial for quantifying the effects of such imperfections. However, conventional interference analyses often assume ideal conditions and overlook transmitter-specific anomalies like carrier leakage, necessitating refined methodologies for accurate performance assessment[12][13].

This paper focuses on evaluating the impact of incompletely suppressed carriers on NavIC signals. It introduces a system model for a homodyne transmitter that incorporates carrier leakage effects into the mathematical representation of NavIC’s interplex signals. The interference is analyzed using metrics such as the SSC and signal-to-noise ratio (SNR) degradation, with a particular emphasis on data demodulation thresholds at the receiver. These insights are vital for optimizing modulator designs, improving interference mitigation strategies, and ensuring the robustness and accuracy of NavIC services in various operational environments. The next section outlines the basic problem formulation, followed by a section that presents models for the interference effects of carrier leakage. Subsequent sections provide numerical examples and conclude with a summary of the findings.

2. Navigation Payload Architecture

The architecture of the navigation payload for the NVS-01 satellite of NavIC is illustrated in Figure 1. This payload is designed to support standard positioning and restricted signal positioning services in the L1, L5, and S bands, with restricted services available in the L5 and S band.

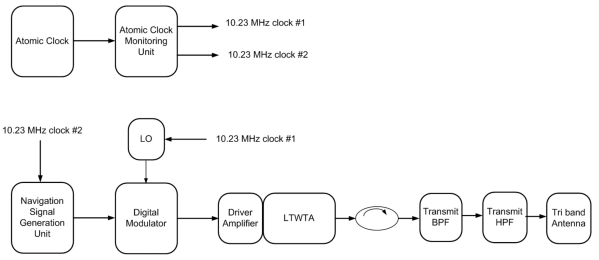

Figure 1. NavIC Navigation Payload architecture (NVS-01)

The Navigation Signal Generation Unit (NSGU) performs several important functions: it receives, stores, extracts, and formats broadcast data. Additionally, it appends the onboard timing information and transmits the processed data to the onboard modulators.

In the NavIC satellite, there are three distinct modulators used for translating baseband navigation signals to RF navigation signals each for the L1, L5, and S band. These modulators utilize homodyne architecture with translation from zero-IF to RF, easing the filter requirements. These modulators utilize ”Synthesized Binary Offset Carrier” and “Interplex” modulations in L1 and L5/S bands to multiplex various navigation signals, resulting in a constant envelope composite signal. This modulated signal is then amplified by a Linearized Traveling Wave Tube Amplifier (LTWTA) and transmitted using a Tri-band Shared Aperture Patch Array antenna.

3. L5 and S Band Signals Description and INTERPLEX Multiplexing Scheme

The mathematical definition of baseband navigation signals for L5 and S-band payloads is based on the symbol definitions provided in Table 1 and equation Equation 1 to Equation 6.

1. **SPS Data Signal**

doi.org/10.32388/U517J4.3

$$s_{\mathrm{SPS}}(t) \tag{1}$$
$$= \sum_{i=-\infty}^{\infty} c_{\mathrm{SPS}}\left(|i|_{L_{\mathrm{SPS}}}\right) d_{\mathrm{SPS}}\left(|i|_{CD_{\mathrm{SPS}}}\right) \mathrm{rect}_{T_{c,\mathrm{SPS}}}\left(t - iT_{c,\mathrm{SPS}}\right)$$

2. **RS Pilot Signal**

$$s_{\mathrm{RSP}}(t) \tag{2}$$
$$= \sum_{i=-\infty}^{\infty} c_{\mathrm{RSP}}\left(|i|_{L_{\mathrm{RSP}}}\right) \mathrm{rect}_{T_{c,\mathrm{RSP}}}\left(t - iT_{c,\mathrm{RSP}}\right) SC_{\mathrm{RSP}}(t,0)$$

3. **RS Data Signal**

$$s_{\mathrm{RSD}}(t) \tag{3}$$
$$= \sum_{i=-\infty}^{\infty} c_{\mathrm{RSD}}\left(|i|_{L_{\mathrm{RSD}}}\right) \mathrm{rect}_{T_{c,\mathrm{RSD}}}\left(t - iT_{c,\mathrm{RSD}}\right) SC_{\mathrm{RSD}}(t,0)$$

The sub-carrier is defined as:

$$SC_{\mathrm{x}}(t,\phi) = \mathrm{sgn}[\sin\left(2\pi f_{SC,x} t + \phi\right)] \tag{4}$$

The NVS-01 RS data and pilot BOC signals are sinBOC, meaning the subcarrier $\phi = 0$. The complex envelope of the composite signal with the Interplex signal $I(t)$ is:

doi.org/10.32388/U517J4.3

$$s(t) = \frac{1}{3}[\sqrt{2}[(s_{SPS}(t) + s_{RSP}(t)) + j(2 \cdot s_{RSD}(t) - I(t))] \quad (5)$$

According to Equation 5, the band-pass representation of the composite modulated navigation signal $S_{\mathrm{RF}}(t)$ at L5, and S band is defined as follows:

$$S_{RF}(t) = S_i(t)\cos\left(2\pi f_{\text{L5 or S}}(t)\right) + S_q(t)\sin\left(2\pi f_{\text{L5 or S}}(t)\right) \tag{6}$$

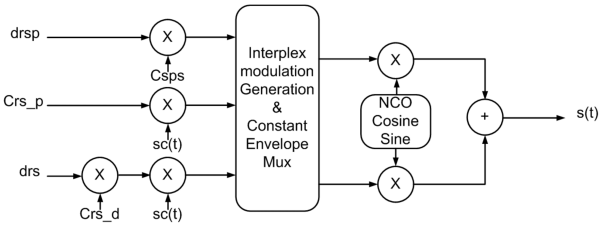

Figure 2. Block schematic for composite signal generation

The operation $|i|x$ provides the code chip index for any signal, while $[i]x$ gives the data bit index for the same signal. Table 2 presents the data rates, code rates, and subcarrier rates for composite signal generation. A block schematic illustrating the composite signal generation process is shown in Figure 2.

doi.org/10.32388/U517J4.3

Symbol	Description
$C_x(i)$	i^{th} chip of spreading code
$d_x(i)$	i^{th} chip of navigation code
$sC_x(t)$	Binary NRZ subcarrier
$\lvert i \rvert_x$	i modulo X
$[i]_x$	Integer part of (i/X)
CD_x	No. of Chips per navigation data bit
L_x	Length of spreading code in chips
$rect_x(t)$	Rectangular pulse function with duration x
$T_{c,x}$	Spreading code chip duration
f_{sc}	Sub carrier frequency for interplex signal = 5.115 MHz
ϕ	Subcarrier phase

Table 1. Symbol Definition

doi.org/10.32388/U517J4.3

Parameter	Unit	Value	Description
R_{d_sps}	bps	25	SPS Data Rate
$R_{d\_rs\_d}$	bps	25	RS Data Rate (Legacy Short Code)
		50	RS Data Rate (Legacy Long Code)
R_{c_sps}	Mcpc	1.023	SPS Code Chip Rate
$R_{c\_rs\_d}$	bps	2.046	RS (Data) Code Chip Rate
$R_{c\_rs\_p}$	bps	2.046	RS (Pilot) Code Chip Rate
R_{sc}	MHz	5.115	Sub carrier frequency

Table 2. Parameter Values for Composite SIgnal Generation

4. Principal of Carrier Leakage

The presence of undesirable continuous wave (CW) carriers in the modulated spectrum is referred to as carrier leakage. In the context of the NavIC scenario, a homodyne approach in modulator design is particularly vulnerable to in-band carrier leakage, which cannot be mitigated by onboard filters.

There are at least two ways in which CW leakage can occur at the output. The first is the coupling of the local oscillator (LO) signal from the input port to the output port of the mixer, which is influenced by the isolation between the LO port and the output port of the mixer, as illustrated in Figure 3. The second cause is the DC bias between the digital I and Q signals generated after the digital-to-analog conversion in the modulators. This offset will be unconverted by the mixer, resulting in leakage at the center frequencies of the S, L5 and L1 band spectrum. This phenomenon is illustrated in Figure 4.

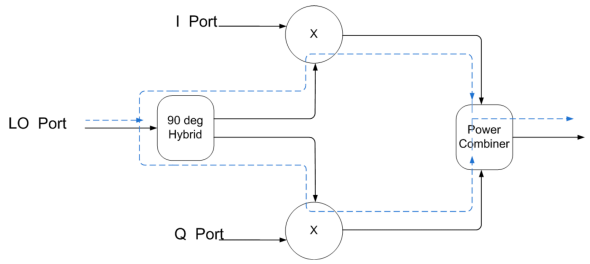

Figure 3. Leakage path in Mixer

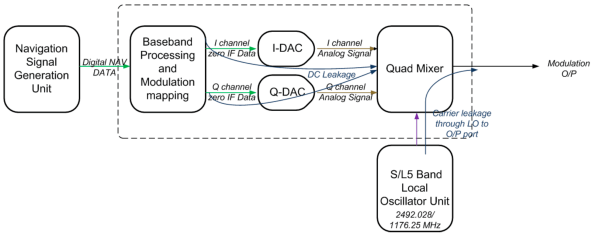

Figure 4. Leakage path in modulator

Taking an Interplex-modulated signal $S(t)$, defined in Equation 6, its carrier leakage generation can be explained using the following equation:

$$S(t) = S_i(t)\cos(2\pi ft + \theta_i) + S_q(t)\sin(2\pi ft + \theta_q) + \beta\cos(2\pi ft + \theta_q) + \gamma\sin(2\pi ft + \theta_i)$$

where, S_i represents the signal from the I channel and S_q represent the signal from the Q channel. The terms β and γ denote the coupling coefficients experienced by the local oscillator (LO) signal in the I channel and Q channel, respectively, at the multiplier within the mixer. Assuming that $\beta = \gamma = \alpha$ and $\theta_i = \theta_q = \theta_\alpha$, the output of the modulated signal can be expressed as follows:

$$S(t) = S_i(t)\cos(2\pi ft + \theta_i) + S_q(t)\sin(2\pi ft + \theta_q) + \sqrt{2}\alpha\sin\left(2\pi ft + \theta_\alpha + \frac{\pi}{4}\right)$$

Figure 5 and Figure 6 show the frequency spectrum and time domain waveform of signals with the leaked carrier.

doi.org/10.32388/U517J4.3

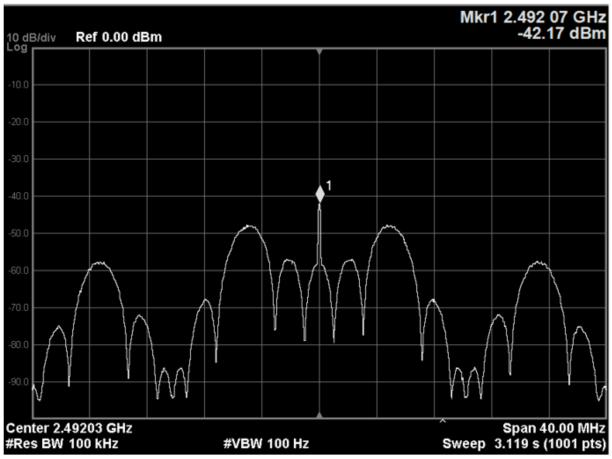

Figure 5. Frequency Spectrum with Carrier Leakage

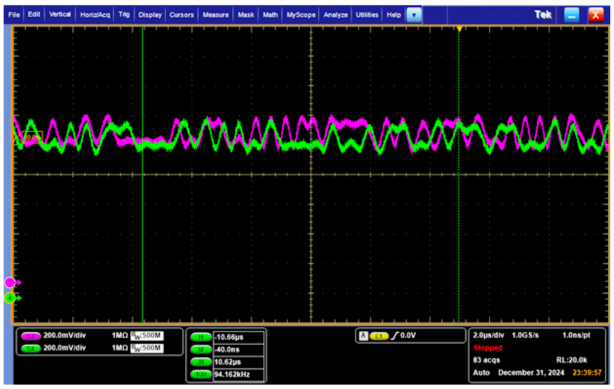

Figure 6. Time domain waveform of I and Q Channel with IQ offset

4.1. Impact of Power Loss

The carrier leakage signal is amplified by the LTWTA, which draws power from the intended signal and generates a spurious signal in the transmitted navigation signal. These effects reduce the effective power available for the intended signal, leading to a degradation in the Signal-to-Noise Ratio (SNR) of the received navigation signal.

Let's define the power of the intended signal as $P_{\text{useful\_power}}$ and the power of the carrier leakage as $P_{\text{carrier\_leakage}}$. The satellite's Effective Isotropic Radiated Power (EIRP) is represented by

$$P_{\text{EIRP}} = P_{\text{useful\_power}} + P_{\text{carrier\_leakage}} \tag{9}$$

and Signal to Noise ratio (SNR) with and without carrier leakage is represented by:

$$SNR_{\text{with carrier leakage}} = \frac{P_{EIRP} - P_{\text{useful\_power}}}{N_0 B} \tag{10}$$

$$SNR_{\text{without carrier leakage}} = \frac{P_{\text{EIRP}}}{N_0 B} \tag{11}$$

Since the P_{EIRP} is fixed and cannot be increased after the satellite configuration is operational, carrier leakage reduces the P_{intended} compared to a scenario where carrier leakage is not present in the system. Additionally, N_0 represents the noise power density per unit bandwidth, while B denotes the NavIC signal bandwidth. The reduction in SNR due to carrier leakage can be calculated using a specific equation.

$$\begin{aligned}&\text{Loss in } SNR \text{ due to carrier leakage} \\ &= SNR_{\text{with carrier leakage}} - SNR_{\text{without carrier leakage}}\end{aligned} \tag{12}$$

4.2. Impact on Data Demodulation

The typical GNSS receiver is shown in Figure 7.

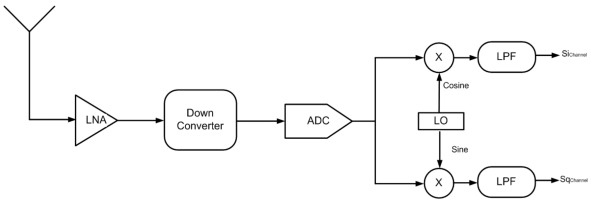

Figure 7. Block Diagram of GNSS Receiver

Assuming ideal channel, the received signal is same as transmitted signal given in Equation 8. The in-phase ($S_{i_{\text{channel}}}$) and quadrature phase ($S_{q_{\text{channel}}}$) outputs for a coherent demodulator using local oscillator with centre frequency f_r and phase θ_r are described in Equation 13.

doi.org/10.32388/U517J4.3

$$\begin{aligned} S_{i_{\text{channel}}} &= \tfrac{1}{2}(S_i(t)\cos(2\pi(f-f_r)t+(\theta_i-\theta_r)) \\ &\quad -S_q(t)\sin(2\pi(f-f_r)t+(\theta_q-\theta_r)) \\ &\quad -\sqrt{2}\alpha\sin(2\pi(f-f_r)t+(\theta_\alpha-\theta_r)+\pi/4)) \\ S_{q_{\text{channel}}} &= \tfrac{1}{2}(-S_i(t)\sin(2\pi(f-f_r)t+(\theta_i-\theta_r)) \\ &\quad +S_q(t)\cos(2\pi(f-f_r)t+(\theta_q-\theta_r) \\ &\quad +\sqrt{2}\alpha\cos(2\pi(f-f_r)t+(\theta_\alpha-\theta_r)+\pi/4)) \end{aligned} \tag{13}$$

After the tracking loop $f \to f_{\text{receiver}}$ and $\theta_i = \theta_q \to \theta_r$, hence:

$$\begin{aligned} S_{i_{\text{channel}}} &= \tfrac{1}{2}(S_i(t)-\sqrt{2}\alpha\sin(\theta_\alpha-\theta_r+\pi/4)) \\ S_{q_{\text{channel}}} &= \tfrac{1}{2}(S_q(t)+\sqrt{2}\alpha\cos(\theta_\alpha-\theta_r+\pi/4)) \end{aligned} \tag{14}$$

We can conclude from the equations above that the carrier leak introduces the DC offset in the I and Q channel output at the receiver, which may affect the data demodulation process.

4.3. Impact on Intersystem/intrasystem Interference

The ITU recommendation M.1831 specifies the total signal-to-noise degradation that a user experiences when interference from other GNSS signals is present[14]. This degradation is quantified using the following equation.

$$\Delta_{dB} = \left[1 + \frac{I_0}{P_0 + N_0}\right] \tag{15}$$

where I_0 represents the external interference, P_0 denotes the intrasystem interference, and N_0 indicates the thermal noise present in the system. The external interference for the intended GNSS signal can be calculated using the following equation.

doi.org/10.32388/U517J4.3

$$P_{0[dB/Hz]} = G_{agg[dB]} + P_{\max\,[dB/Hz]} + SSC_{[dB/Hz]} + L_{x[dB]} \tag{16}$$

In this context, $G_{agg[dB]}$ represents the total gain, taking into account the interference from other GNSS signals within the system being evaluated. The inherent processing loss in the receiver is denoted as $L_{x[dB]}$, while P_{max} refers to the maximum power received by the user. The spectral separation coefficient, $SSC_{[dB/Hz]}$, quantifies the separation between the desired GNSS signal and the interfering GNSS signals. The SSC is the most commonly used parameter for analyzing interference in GNSS signals.

When the SSC value is minimal, a GNSS modulation can support multiple signals for desired transmit power levels. This is due to the fact that smaller SSC values offer better resistance to interference from signals that share the same modulation through code multiple access.

The following provides the definition for the spectral separation coefficient (SSC):

$$k_{SSC} = \int_{-\frac{P_r}{2}}^{\frac{P_r}{2}} \overline{G}_l(f) G_s(f) df \tag{17}$$

where the normalized power spectral density $\overline{G}_l(f)$ and is defined by:

$$\overline{G}_l(f) = \begin{cases} \frac{G_l(f)}{\int_{-P_t/2}^{P_t/2} G_l(f) df} & |f| \le \frac{P_t}{2} \\ 0 & otherwise \end{cases} \tag{18}$$

The normalized power spectral density (PSD) is denoted as $G_s(f)$, where P_t represents the transmitting bandwidth and P_r indicates the receiving front-end bandwidth. Lower values of signal-to-signal coefficient (SSC) suggest that the modulation scheme can accommodate higher data rates by providing sufficient processing gain to reduce multiple-access interference from similar signals. This has been supported by findings showing that for SSC values below -60 dB/Hz, the overall C/No generally decreases by less than 0.1 dB[15].

The combined effect of K sets of intrasystem and intersystem signals on the effective global navigation satellite system (GNSS) composite interference is defined as[4]:

$$I_{GNSS} = \sum_{k=1}^{K} C_k L_{ks} k_{SSC} \tag{19}$$

In this context, L_{ks} represents the realization loss, which is a positive value less than one. It accounts for signal acquisition losses caused by interference. This interference results from the power spectral density (PSD) $G_k(f)$, influenced by processes such as analog-to-digital conversion, digital filtering, and various receiver-specific factors that affect the intended signal with PSD $G_s(f)$. Additionally, C_k denotes the received power of the aggregate interference from all signals characterized by the PSD $G_k(f)$.

The SSC values for the NavIC system are calculated based on the previously mentioned equations for BPSK and BOC(5,2) signals in the L5 band (1575.42 MHz) and the S-band (2492.028 MHz), as detailed in Table 3 and Table 4. These SSC values illustrate the impact of competing navigation signals on NavIC signals.

SSC in L5 Band (dB/Hz)	Interfering Signal	Transmit Bandwidth (MHz)	Receiver Bandwidth (MHz)	NavIC BPSK(1) 24	NavIC BOC(5,2) 24	GPS BPSK(10) 24	Galieo AiltBOC(15,10) 92.07
NavIC	**BPSK(1)**	24	24	-61.78	-77.03	-69.88	-73.38
NavIC	**BOC(5,2)**	24	24	-72.99	-67.73	-72.99	-76.16
GPS	**BPSK(10)**	30.69	24	-71.25	-72.99	-71.25	-76.16
Compass	**BPSK(2)**	20.46	24	-101.25	-99.20	-101.32	-74.53
Compass	**BPSK(10)**	20.46	20.46	-100.56	-89.2	-100.56	-74.57
Compass	**AltBOC(15,10)**	51.15	51.15	-74.32	-75.84	-74.32	-74.12
QZSS	**BPSK(10)**	24	24	-71.13	-72.87	-71.13	-74.57
Gailoeo	**AltBOC(15,10)**	92.07	92.07	-74.68	-76.16	-74.69	-75.07

Table 3. SSC Value for Interference among the L5 Band Signals

doi.org/10.32388/U517J4.3

SSC in S Band (dB/Hz)	Interfering Signal	Transmit Bandwidth (MHz)	Receiver Bandwidth (MHz)	NavIC BPSK(1) 16.5 MHz	NavIC BPSK(5,2) 16.5 MHz
NavIC	**BPSK(1)**	16.5	16.5	-67.77	-77.01
NavIC	**BOC(5,2)**	16.5	16.5	-77.01	-61.74
Compass	**BPSK(4)**	16.5	16.5	-66.21	-66.21
Compass	**BPSK(8)**	16.5	16.5	-68.81	-68.81
Compass	**AltBOC(6,2)**	16.5	16.5	-82.54	-82.54

Table 4. SSC Value for Intrefrence among the S Band Signals

Up to this point, the SSC has been based on an ideal signal scenario that assumes no suppressed carrier leakage in the transmitted GNSS signal. We will now extend the SSC calculation to include scenarios where suppressed carriers are present. In these cases, a narrowband signal component appears at the center frequency of the transmitted signal, indicating the presence of an incompletely suppressed carrier. This phenomenon can be observed in the spectrum of test transmitters, as illustrated in Figure 5.

For example, the BOC (Binary Offset Carrier) signal with a subcarrier frequency of 5×1.023 MHz and a spreading code rate of 2×1.023 MHz, known as BOC(5,2), exhibits this behavior. It is important to note that all satellites within the same constellation display a similar level of incompletely suppressed carriers, meaning both the intended signal and the interfering signals share the same center frequency.

The symbol $G_{n,c}(f)$ represents the normalized power spectral density (PSD) of the total partially suppressed carriers from the satellites in the n^{th} constellation. The SSC for scenarios involving partially suppressed carriers from the constellation, as well as the desired signal, is then given by:

$$k_{n,cs} = \int_{-\frac{P_r}{2}}^{\frac{P_r}{2}} G_{n,c}(f) G_s(f) df \tag{20}$$

This bandwidth of a completely concealed carrier is typically substantially smaller than the desired signal's spreading code rate. The SSC (5) in this instance can be roughly described as

$$K_{n,c} \approx \max\left(G_S(0), \phi\right) \tag{21}$$

where ϕ is a receiver-imposed minimum limit caused due to phase noise or other considerations.

When evaluating interference, the significance of incompletely suppressed carrier increases when the interfering signal possesses unbiased modulations like BOC.

5. Effect of Carrier leakage in NavIC scenario

5.1. L5 Band Scenario

In the NavIC navigation satellite series, BPSK(1) and BOC(5,2) modulations are used to transmit data for various services in the L5 band. Let's consider a scenario with interference in NavIC, where the interfering signals employ BOC(5,2) modulation while the desired signal uses BPSK(1) modulation with a spreading code of 1.023 MHz. The power of the interfering signal has a normalized bandwidth of $(24 \times 1.023\text{MHz})$, and the receiver operates with a rectangular passband of 24 MHz. According to Table 3, the Spectral Separation Coefficient (SSC) between the interfering and desired signals is -77.03 dB/Hz. Applying Equation Equation 20 and Equation 21 in the L5 scenario, the SSC between the partly suppressed carrier of BOC(5,2) interference and the desired signal is -60.1 dB/Hz.

When the power of the incompletely suppressed carrier is sufficiently low, the BOC(5,2) interference mainly dictates the SSC, with the SSC of the partially suppressed carrier being 17 dB higher than that of the interference. As a result, the effect of the partly suppressed carrier is negligible if its power is 27 dB below the interference power of BOC (5,2) or 10 dB below the point where its SSC exceeds that of the interference.

Similarly, as shown in Table Table 3, the worst-case SSC is -61.78 dB/Hz, where BPSK(1) from another satellite interferes with the desired BPSK(1) signal. In this scenario, when the power of the incompletely suppressed

doi.org/10.32388/U517J4.3

carrier is 10 dB lower than the threshold at which its SSC exceeds that of the BPSK(1) interference, or 11 dB below the interference power, the impact of the partially suppressed carrier is minimal. Here, the SSC of the partially suppressed carrier is 1 dB higher than that of the interference.

Figure 8 illustrates the performance of a received BPSK(1) signal with a signal strength of -158.5 dBW, thermal noise power of -201.5 dBW / Hz and cumulative interference of BOC (5,2)(5,2) at various power levels along with different levels of carrier suppression. This analysis assumes that only intrasystem-suppressed carrier interference is present at the center frequency band, targeting the signal. The results confirm that the inadequately suppressed carrier has a negligible effect on C/N_0eff when the carrier suppression is 27 dB or more below the interference power of BOC (5,2).

Figure 9 presents an analysis of the desired BPSK(1) signal with aggregate BPSK(1) interference at different power levels and carrier suppression levels. The numerical results confirm that when the carrier is suppressed by 11 dB below the interference power of BPSK (1), the partially suppressed carrier has a negligible impact on C/N_0eff.

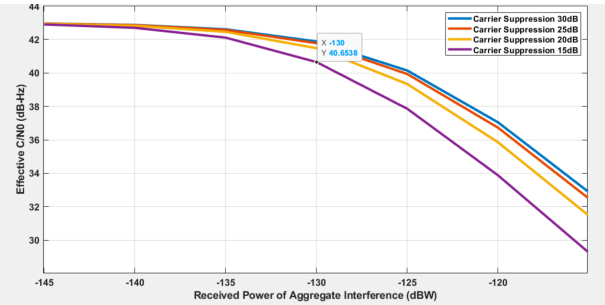

Figure 8. Effect of C/N0 with respect to carrier separation L5-band NavIC Signal (BPSK(1) Desired Signal with BOC(5,2))

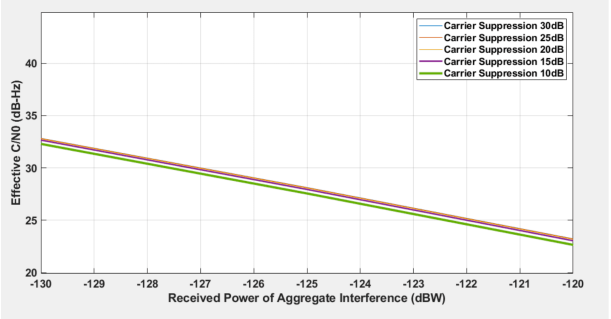

Figure 9. Effect of C/N0 with respect to carrier separation L5-band NavIC Signal (BPSK(1) Desired Signal with BPSK(1)

In the NavIC series of navigation satellites, the modulations BPSK (1) and BOC (5,2) are utilized to transmit data for various services in the S band, similar to the L5 band. Consider a scenario in which interference signals employ BOC (5,2) modulation, similar to that in the L5 band, while the desired signal uses BPSK(1) modulation with a spreading code rate of 1×1.023MHz. According to Table 4, the signal-to-interference ratio (SIR) for interference signals is -77.01 dB/Hz, normalized over a bandwidth of 168.795 MHz, with the receiver using a 16.5 MHz rectangular passband.

The Signal-to-Interference Ratio for the desired BPSK(1) signal and the partially suppressed carrier interference of BOC (5,2) is calculated to be -60.1 dB/Hz, based on Equation (6). The behavior of BOC (5,2) interference in BPSK (1) in the S band mirrors its effects in the L5 band, where interference remains dominant as long as the power of the partially suppressed carrier is significantly lower than that of the primary interference.

As indicated in Table 4, the worst-case SIR is -67.77 dB/Hz, where the desired BPSK(1) signal is interfered with by another satellite's BPSK(1) signal. When the power of the incompletely suppressed carrier is 10 dB lower than the threshold at which its SIR exceeds that of the BPSK(1) interference, or 17 dB below the interference power of BPSK(1), the impact of the partially suppressed carrier is expected to be negligible. In this scenario, the SIR of the incompletely suppressed carrier is 7 dB higher than that of the interference.

The results for the desired BPSK(1) signal, obtained at a power level of -158.5 dBW, with thermal noise at -201.5 dBW/Hz and aggregate BPSK(1) interference at varying signal power levels and different carrier suppression levels, are presented in Figure 10. This hypothetical case assumes the absence of external interference, including signals that share the same frequency spectrum as the target signal. The numerical findings confirm that even

doi.org/10.32388/U517J4.3

without external interference to obscure the effects, the inadequately suppressed carrier contributes negligibly to $((C/N_0)_{\text{eff}}$ when the carrier is suppressed by 17 dB or more below the interference power of BPSK (1).

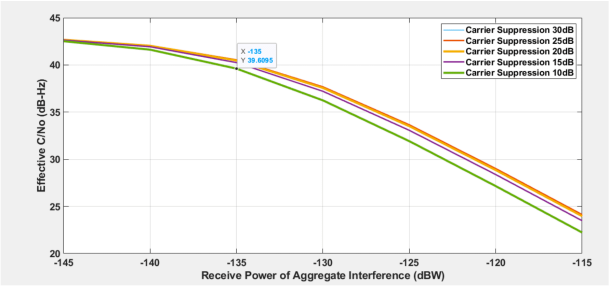

Figure 10. Effect of C/N0 with respect to carrier separation for S-band NavIC Signal (BPSK(1) Desired Signal with BPSK(1)

By measuring the power of the poorly suppressed carriers sent by satellites in a constellation, the effect of an underlying carrier on both intersystem and intrasystem communication can be assessed for each constellation.

6. Degradation in Effective Transmitted Power

In NavIC satellites, the onboard suppressed carrier is amplified by both the drive amplifier and the LTWTA. This process consumes power from these amplifiers and reduces the effective transmitted power of the desired signal. A critical factor affecting this power allocation is the difference between the power of the desired signal and the power associated with the suppressed carrier.

For PSK (Phase Shift Keying) modulation, which is commonly used in GNSS and NavIC systems, unwanted RF power can result from components at the carrier frequency within the modulated spectrum. This leakage negatively affects the power efficiency of the transmitted signal.

Table 5 illustrates the effect of carrier separation on a 250 W linearized LTWTA with a saturated gain of 50 dB. The findings indicate that carrier separation values greater than 24 dB have minimal effect on total transmitted power. However, when the separation decreases to 20 dB or below, the suppressed carrier consumes more than 2 W of the total transmitted power. This excessive consumption emphasizes the need to maintain carrier separation above 20 dB to optimize power efficiency.

Similarly, Table 6 shows that in the L5 band, carrier separation below 20 dB reduces the desired signal power by approximately 1.4 W. Although this reduction is less severe than the power loss observed in the S-band, it still has a significant impact on the overall transmission output.

While occasional increases in carrier leakage may not pose a serious threat—assuming that carrier suppression remains above 20 dB—other factors can further degrade system performance. Parameters such as rise and fall times, data asymmetry, and band-limiting effects can significantly influence overall signal quality beyond the impact of carrier leakage alone. Therefore, while ensuring adequate carrier suppression is crucial, addressing these additional factors is equally important for maintaining optimal performance in NavIC systems.

doi.org/10.32388/U517J4.3

Carrier Separation	dB	30	24	20	18
Total Saturated Power	dBm	54	54	54	54
Gain at Saturation of LTWTA	dB	50	50	50	50
Useful Power	Watt	249.75	249.01	247.52	246.09
Power Loss	Watt	0.25	0.99	2.47	3.9

Table 5. Estimated Degradation due to Carrier Separation in S-Band NavIC signal

doi.org/10.32388/U517J4.3

Carrier Separation	dB	30	24	20	18
Total Saturated Power	dBm	54	54	54	54
Gain at Saturation of LTWTA	dB	50	50	50	50
Useful Power	Watt	149.85	149.40	148.52	147.65
Power Loss	Watt	0.15	0.59	1.48	2.34

Table 6. Estimated Degradation due to Carrier Separation in L5 Band NavIC signal

7. Conclusion

The research presents an improved technique for evaluating RF interference in NavIC systems, particularly focusing on inadequately suppressed carriers. This enhancement allows for the definition of additional spectral separation coefficients that consider the effects of these imperfections.

The model for imperfections enables a more thorough evaluation of both intrasystem and intersystem interference, taking into account real-world conditions where satellite transmitters may exhibit varying levels of signal imperfections. Mathematical analysis shows that signals with different modulation types display different sensitivities to these imperfections. In instances where satellite transmitters have minimal signal imperfections, evaluations based solely on idealized signals may suffice. However, as the level of signal imperfections increases, it becomes essential to consider them when assessing interference. The study also highlights the impact of carrier leakage on data demodulation thresholds, noting that higher levels of leakage significantly affect performance.

This methodology provides valuable insights into the acceptable thresholds for signal imperfections in future NavIC systems. By incorporating these imperfections into interference assessments, designers can improve their understanding and management of potential interference issues, ultimately enhancing the reliability and performance of NavIC systems.

[16][17].

Statements and Declarations

Availability of data and materials

All relevant data are provided in the paper.

Conflicts of interest

The authors declare no conflict of interest and no competing interest.

Funding

The work is supported under the ISRO navigation program

Authors' contributions

Deepak Mishra: Conceptualization, Formal analysis, Methodology, Project administration, Supervision, Validation, Writing – review & editing, Writing – original draft. Neeraj Mishra: Conceptualization, Data curation, Formal analysis, Methodology, Software, Writing – original draft, Writing – review & editing. Harsh Agarwal: Methodology, Validation, Writing – review & editing

Acknowledgments

We acknowledge Space Applications Centre, Indian Space Research Organization and Department of Space, Government of India for funding this project and providing all the required resources.

References

1. ^*Pany T, Akos D, Arribas J, Bhuiyan MZH, Closas P, Dovis F, Fernandez-Hernandez I, Fern⊠ndez⊠0Prades C, Gun awardena S, Humphreys T, Kassas ZM, L⊠3pez Salcedo JA, Nicola M, Psiaki ML, R⊠bgamer A, Song Y, Won J (20 24). "GNSS software-defined radio: history, current devel opments, and standardization efforts". Institute of Navig ation. 71 (1): 173⊠0196.*
2. ^*Hein GW (2020). "Status perspectives and trends of sat ellite navigations". Satellite Navigation. 1 (22).*
3. ^*Zangenehnejad FG (2021). "GNSS smartphones positio ning: advances, challenges, opportunities, and future per spectives". Satellite Navigation. 2 (24).*

4. a, b Sura P (2023). "NavIC and gagan". Proceedings of the 36th International Technical Meeting of the Satellite Division of The Institute of Navigation (ION GNSS+ 2023), Denver, Colorado, September 2023, pp. 1053–1063. doi:10.33012/2023.19200.
5. ^ Steigenberger JS, Montenbruck O (2023). "New navic clock outperforms previous generation". GPS World. 34 (9): 12+.
6. ^ Betz JW, T. B.M. (1978). "Intersystem and intrasystem interference with signal imperfections". Proceeding of Position Location and Navigation Symposium, Monterey, CA, USA, 26–29 April 2004.
7. ^ Enneking C (2020). "Intra- and intersystem interference in gnss: performance models and signal design". Note: 108 f. Tese (doutorado) - Universidade Federal do Ceará, Centro de Tecnologia, Pro-grama de Pós-Gradua–ão em Engenharia de Teleinformática, Fortaleza.
8. ^ Betz JW (2000). "Effect of narrowband interference on gps code tracking accuracy". Proceedings of ION 2000 National Technical Meeting, Institute of Navigation, January 2000.
9. ^ He LX, C.Y. (2012). "The impact of carrier leakage and spectral asymmetry distortions on the performance of navigation signals". Proeeding of China Satellite, Navition Conference.
10. ^ Phelts WT, Walter RE, E. P (2003). "Toward real-time sqm for waas: improved detection techniques". Proceeding ION GNSS, pp. 2739–03749.
11. ^ He LX, C.Y., Lu J (2015). "Generation mechanisms of gnss navigation signal distortions and influence on ranging performance". Systems Engineering and Electronics. 37: 1611–01620.
12. ^ Mishra SB, Bhatnagar S (2018). "Evaluation of intersystem interference between navic, gps and galileo". Communications on Applied Electronics. 7 (12): 7–011.
13. ^ Titus CJHB, Owen R (2003). "Intersystem and intrasystem interference analysis methodology". Proceedings of / ON GNSS-2003, Institute of Navigation, September 2003.
14. ^ ITU (Ed.) (2015). "A coordination methodology for radionavigation-satellite service inter-system interference estimation (recommendation itu-r m.1831-1)". ITU, Geneva, Switzerland.
15. ^ Betz JW, Kolodziejski KR (October 2009). "Generalized theory of code tracking with an early-late discriminator part ii: noncoherent processing and numerical results". IEEE Transactions on Aerospace and Electronic System. 45 (4): 1557–01564.
16. ^ Rebeyrol LR, Issler JL, Bousquet M, Boucheret M-L (2006). "Interplex modulation for navigation systems at the l1 band". Proceedings of the 2006 National Technical Meeting of The Institute of Navigation, Monterey, CA, January 2006, pp. 100–0111.
17. ^ Upadhyay DJ, Bhadouria VS, Majithiya PJ, Bera SC (2024). "Synthesized binary offset carrier modulation for interoperable gnss l1 band signals". Institute of Navigation. 71 (2).

Declarations

Funding: The work is supported under the ISRO navigation program.
Potential competing interests: No potential competing interests to declare.